

Submodular Optimization for Voltage Control

Zhipeng Liu, *Student Member, IEEE*, Andrew Clark, *Member, IEEE*, Phillip Lee, *Member, IEEE*, Linda Bushnell, *Fellow, IEEE*, Daniel Kirschen, *Fellow, IEEE*, and Radha Poovendran, *Fellow, IEEE*

Abstract—Voltage instability occurs when a power system is unable to meet the reactive power demand, and is typically corrected by switching on additional reactive power devices such as capacitor banks. Real-time monitoring and communication technologies can potentially improve voltage stability by enabling the rapid detection of low voltages and the implementation of corrective actions. These corrective actions, however, will only be effective in restoring stability if they are chosen in a timely, scalable manner. In this paper, we propose a submodular optimization approach for designing a control strategy that prevents voltage instability. Our key insight is that the voltage deviation from the desired level is a supermodular function of the set of reactive power injections that are employed, leading to computationally efficient control algorithms for stabilization with provable optimality guarantees. This submodular control framework is tested on the IEEE 300-bus transmission system.

Index Terms—Voltage stability, voltage control, submodular optimization.

I. INTRODUCTION

Voltage stability refers to the ability of a power system to maintain acceptable voltages under normal conditions and after disturbances [1]. The inability to prevent system voltages from decreasing uncontrollably (voltage collapse) has resulted in extensive blackouts, including the 2003 Northeast US blackout, 1983 Sweden power outage, and 1987 Tokyo blackout [2]. Voltage instability occurs when a power system is unable to meet the reactive power demand, and is typically corrected by injecting reactive power at some buses using capacitor/reactor bank switching or transformer tap changing [1]. In order to limit the complexity associated with coordinating actions taken over large networks by multiple system operators, these corrective actions are traditionally performed as local controls [3]. A purely local approach that does not take the interactions between neighboring buses into account, however, may be insufficient to meet reactive power demands when voltage deviations occur simultaneously at multiple buses.

Enhanced monitoring and communication capabilities could help improve voltage stability by enabling centralized or hierarchical controls. One such architecture was proposed in [4], and is currently being implemented in southern California. Under this approach, voltage magnitudes and phase angles are measured using Phasor Measurement Units (PMUs). These measurements are used to evaluate the effectiveness

of distributed voltage controls and, when necessary, devise a coordinated, centralized response.

A crucial step in a coordinated response is selecting a set of control actions based on the state of the system. If the set of actions at each bus is discrete (e.g., switch a capacitor bank on or off), designing a centralized control response to resolve multiple voltage deviations is a discrete subset selection problem. At present, such actions are heuristically chosen via enumeration and evaluation of combinations of control actions at multiple buses, after pruning the search space of all possible combinations using human expert domain knowledge [4]. Since the computation time of this approach is worst-case exponential in the number of buses, it does not scale to large power systems. Furthermore, it may result in a suboptimal response or fail to timely identify a set of control actions to prevent an impending voltage collapse. A computationally efficient optimization approach that exploits the underlying structure of the voltage regulation problem to select provably optimal control actions is thus needed to enable a timely and effective coordinated response to voltage instability.

This paper presents such an approach, namely a submodular optimization approach to voltage control in power systems. Submodularity is a diminishing returns property of set functions that enables the development of efficient approximation algorithms. Our fundamental insight is that the metrics typically used to evaluate the effectiveness of a voltage control strategy, such as the deviation from the desired voltage and the capacitor/reactor switching cost, have an inherent submodular structure. We make the following specific contributions:

- We formulate the problem of selecting a set of reactive power injection devices to minimize the deviation of the voltages from their desired values and the total operating cost. We prove that this problem is equivalent to submodular maximization with a matroid basis constraint.
- We propose polynomial-time algorithms for computing the optimal voltage control strategy. The performance of a control strategy is measured by its total operating costs plus remaining voltage deviations after control. We prove that the control strategies returned by our algorithms have performance no worse than a factor $1/3$ of the optimal control strategy.
- We present both a non-adaptive algorithm, which assumes that switching each reactive device results in a fixed change in system voltages based on the initial system operating point, as well as an adaptive algorithm that updates the operating point after each selection.
- We evaluate our submodular approach through a numerical study on the IEEE 300-bus test system. We find that, within the same computational time, our approach results in voltage

Manuscript received August XX, 2016; revised Jan XX, 2017.

Z. Liu, P. Lee, L. Bushnell, D. Kirschen and R. Poovendran are with the Department of Electrical Engineering, University of Washington, Seattle, WA, 98195 USA (e-mail: {zhipliu, leep3, lb2, kirschen, rp3}@uw.edu).

A. Clark is with the Department of Electrical and Computer Engineering, Worcester Polytechnic Institute, Worcester, MA 01609 USA (e-mail: aclark@wpi.edu).

This work was supported by NSF grant CNS-1544173.

profiles with less deviation compared to a state-of-the-art algorithm that searches over a subset of the possible control actions based on voltage sensitivities to reactive power injections.

The rest of this paper is organized as follows. Section II reviews related work. Section III presents the power system model used for voltage control and provides background information on submodularity. Section IV presents the problem formulation and the approximation algorithms based on submodular optimization. Section V presents the simulation results. Section VI concludes the paper.

II. RELATED WORK

The study of voltage instability problems dates back to the 1980s. Dobson and Chiang [5] introduced a model of voltage collapse that identifies the point of bifurcation as the operating point leading to voltage collapse. Traditional approaches to mitigating voltage instability are mainly preventive actions based on contingency ranking [6].

In the early 1990s, a three-level hierarchical voltage control scheme was proposed and later implemented in several European countries [7], [8], [9], [10]. The idea is analogous to the hierarchical levels of frequency control. In these schemes, a “pilot bus” that represents the voltage profile of a given region is selected and all control actions aim at regulating the voltage at this bus. Ongoing research address the pilot bus selection problem with improvements mostly in selection theory and decentralization of the controller [11].

Selecting a pilot point or a control region that is loosely coupled to the rest of the system is difficult. Furthermore, in North America, most voltage control actions are achieved by switching in or out capacitor or reactor banks. An on-line voltage regulation approach was proposed in [12] based on capacitor switching and power generation resetting. This approach, however, is limited in practice because operators hesitate to switch capacitor banks frequently. A slow centralized online voltage control scheme was proposed in [13] and further improved in [14]. In [13], the controller utilizes SCADA measurements and state estimation to predict the incremental effects of a switching action. The goal is to resolve any voltage violation with minimum switching actions and circular reactive flows. In [14], the state estimator is replaced by an integer programming method for deciding switching actions directly from the SCADA data and hence the computational overhead is significantly reduced. These approaches, however, are based on the assumption that the problematic areas containing voltage violations are loosely coupled and can be considered as separate control regions. When buses with voltage violations are closely coupled, the computational burden of these proposed methods either increases exponentially or the optimality deteriorates because the size of the control area is reduced.

Recently, a hierarchical, centralized strategy that addresses the voltage regulation problem for large power systems was proposed in [4]. In this approach, reactive power control is exerted through switching of reactive power injection devices to regulate voltage while minimizing the operating costs. This approach requires an enumeration of all possible configurations

of reactive devices. To keep this enumeration computationally tractable, the system is partitioned into small areas and the enumeration is done within each area. This partitioning does not take into account the interactions between the voltages in the various areas and thus makes the solutions suboptimal.

Distributed or decentralized approaches for voltage regulation based on control theory are presented in [3], [15]. Zhang et al. [3] identify a sufficient condition for regulating voltage in a distributed manner with limited communication between buses. Robbins et al. [15] derive a distributed control law that guarantees voltage stability by varying the reactive power injection at each bus using distributed energy resources (DER). These works assume that the reactive power injection at every bus can be dynamically adjusted and do not take into account the associated cost.

Other voltage control approaches based on wide-area measurements are described in [16], [17], [18]. The control schemes in [16] and [17] rely on a constrained optimization, which is solved using linear or stochastic programming depending on the model used. In [18], a real-time control scheme is proposed to assess the power system stress and adjust voltage control actions for different stressed situations. These approaches, however, mainly rely on the control of generator voltage setpoints and load shedding, which are not suited to the deregulated power systems of the North American power grid where operators do not have direct control over generators.

Submodular optimization techniques for control of networked systems have been proposed in [19], [20]. These techniques focus on optimizing performance parameters, such as robustness to noise, smooth convergence, and controllability of linear systems. At present, however, submodularity has not been explored in the context of power system stability and control. This paper adds an adaptive-selection algorithm to the preliminary version [21] and has a detailed validation of proposed control algorithms on a larger power system.

III. SYSTEM MODEL AND PRELIMINARIES

In this section, we present the power system model and introduce notations that will be used throughout the paper. We also give a background on submodularity.

A. Power System Model

We consider a power system consisting of n PQ buses, m PV buses and a slack bus. We index PQ buses by $i = 1, \dots, n$, PV buses by $i = n + 1, \dots, n + m$ and the slack bus by $i = 0$. At each bus i , the voltage magnitude V_i and angle θ_i can be measured by PMUs and are available to the centralized controller. A set of capacitor and reactor banks, denoted as Ω , is located at a subset of PQ buses. One PQ bus i may have multiple capacitor/reactor banks, denoted as Ω_i , available to switch in or out. Switching a capacitor/reactor bank $j \in \Omega_i$ located at bus i increases the reactive power injection at bus i by ΔQ_j . The magnitude of the change is taken to be a function of pre-switching voltage at the bus where the capacitor/reactor bank is located, e.g., $|\Delta Q_j| = C_j V_i^2$, where C_j is the capacitance of the capacitor/reactor bank j . If a subset of capacitor/reactor banks, $S_i \subseteq \Omega_i$, are switched at

bus i , then the total change in reactive power injection at bus i is the sum of changes due to individual switches, denoted as $(\Delta Q)_i = \sum_{j \in S_i} \Delta Q_j$.

The impact of reactive power injection on the system voltages is derived as follows using a linearization of the power flow equations. We denote the admittance of the transmission line between bus i and j as $y_{ij} = g_{ij} - jb_{ij}$ where g_{ij} and b_{ij} denote the conductance and susceptance, respectively. Note that $g_{ii} = -\sum_{j \neq i}^{n+m} g_{ij}$ and $b_{ii} = -\sum_{j \neq i}^{n+m} b_{ij}$. At each bus i , the active power injection P_i and reactive power injection Q_i satisfy the power flow equations

$$P_i = V_i \sum_{j=0}^{n+m} V_j [g_{ij} \cos(\theta_i - \theta_j) + b_{ij} \sin(\theta_i - \theta_j)], \quad (1)$$

$$Q_i = V_i \sum_{j=0}^{n+m} V_j [g_{ij} \sin(\theta_i - \theta_j) - b_{ij} \cos(\theta_i - \theta_j)]. \quad (2)$$

Define $P = [P_1, P_2, \dots, P_{n+m}]^T$ as the vector of active power injections at all PQ and PV buses and $Q = [Q_1, Q_2, \dots, Q_n]^T$ as the vector of reactive power injections at PQ buses. By linearizing these equations around the current operating point, we obtain the following relation that contains a Jacobian matrix, J , of power flow equations, $[\Delta P^T \ \Delta Q^T]^T = J[\Delta \theta^T \ \Delta V^T]^T$, where $\Delta P = [(\Delta P)_1, (\Delta P)_2, \dots, (\Delta P)_{n+m}]^T$ is the vector of changes in active power injections at PQ and PV buses, while $\Delta Q = [(\Delta Q)_1, (\Delta Q)_2, \dots, (\Delta Q)_n]^T$ is the vector of changes in reactive power injections at PQ buses. The vector $\Delta \theta = [\Delta \theta_1, \Delta \theta_2, \dots, \Delta \theta_{n+m}]^T$ refers to changes in bus angles at PQ and PV buses, while $\Delta V = [\Delta V_1, \Delta V_2, \dots, \Delta V_n]^T$ refers to changes in voltage magnitudes at PQ buses.

The Jacobian matrix J is assumed to be invertible under normal operating condition. This assumption is consistent with existing literature [5], [22], where the operating point at which the Jacobian matrix J becomes singular was identified as the point of voltage collapse since no change in power injection could stabilize the change in voltage magnitudes.

Inverting the matrix J and using the fact that the changes in real power injections are zero ($\Delta P = 0$) implies that voltage changes at all PQ buses due to capacitor/reactor bank switches can be approximated by

$$\Delta V = D \Delta Q, \quad (3)$$

where D is the $n \times n$ sub matrix of J^{-1} describing the effect of changes in reactive power injections on changes in voltage magnitudes.

B. Background on Submodularity

Submodularity is a diminishing returns property of set functions, wherein the incremental benefit of adding an element to a set S decreases as more elements are added to S . It is analogous to concavity of continuous functions. The following formally defines submodularity.

Definition 1 ([23]). *Let V be a finite set, and let 2^V denote the set of all subsets of V (power set). A function $f : 2^V \rightarrow \mathbb{R}$ is submodular if, for any subsets $S \subseteq V$ and $T \subseteq V$,*

$$f(S) + f(T) \geq f(S \cup T) + f(S \cap T). \quad (4)$$

In addition, f is supermodular if $-f$ is submodular. f is modular if the equality holds in (4).

It can be shown that a nonnegative weighted sum of submodular functions is submodular. As a notation, let $|S|$ denote the cardinality of a set S . A matroid is defined as follows.

Definition 2. *Let V be a finite set, and let \mathcal{I} be a collection of subsets of V . The pair $\mathcal{M} = (V, \mathcal{I})$ is a matroid if the following three conditions hold: (i) $\emptyset \in \mathcal{I}$, (ii) If $B \in \mathcal{I}$, then $A \in \mathcal{I}$ for all $A \subseteq B$, and (iii) If $A, B \in \mathcal{I}$ and $|A| < |B|$, then there exists $v \in B \setminus A$ such that $(A \cup \{v\}) \in \mathcal{I}$.*

The collection \mathcal{I} is referred to as the set of *independent sets* of the matroid \mathcal{M} . A maximal independent set is a *basis*. It can be shown that all bases of a matroid have the same cardinality. The following lemma defines a sub-class of matroids.

Lemma 1. *Let V denote a finite set, and let V_1, \dots, V_m be a partition of V , i.e., a collection of sets such that $V_1 \cup \dots \cup V_m = V$ and $V_i \cap V_j = \emptyset$ for $i \neq j$. Let d_1, \dots, d_m be a collection of nonnegative integers. Define a set \mathcal{I} by $A \in \mathcal{I}$ iff $|A \cap V_i| \leq d_i$ for all $i = 1, \dots, m$. Then $\mathcal{M} = (V, \mathcal{I})$ is a matroid.*

A matroid defined as in Lemma 1 is a *partition matroid*. The following lemma gives a property of submodular functions over matroid bases.

Lemma 2 ([24]). *Let $\mathcal{M} = (V, \mathcal{I})$ be a matroid, and let $f : 2^V \rightarrow \mathbb{R}$ be a submodular function defined on V . Define S to be a matroid basis such that, for all u and v with $u \in S$, $v \notin S$, and $(S \setminus \{u\} \cup \{v\}) \in \mathcal{I}$, $(1 + \epsilon)f(S) \geq f(S \setminus \{u\} \cup \{v\})$. Then for any basis C of \mathcal{M} ,*

$$2(1 + \epsilon)f(S) \geq f(S \cup C) + f(S \cap C). \quad (5)$$

IV. VOLTAGE CONTROL FRAMEWORK

This section formulates the problem of minimizing the deviation from the desired voltage and the operating cost by selecting a set of reactive power injection devices. We first formulate the problem and prove that it satisfies submodularity. Based on the submodularity property, we present a polynomial-time voltage control algorithm with provable optimality guarantees. We then describe an adaptive selection procedure added to the submodular control algorithm that mitigates the error in state prediction due to linearization.

A. Problem Formulation

A centralized voltage controller can monitor and control the voltages continuously for all PQ buses. In a well-maintained power system, the voltage magnitude typically varies within 5% of the nominal value, e.g., 0.95 ~ 1.05 p.u. (per unit).

Switching a capacitor/reactor bank incurs an operating cost. We denote c_i as the operating cost of switching in a capacitor bank i that is inactive or switching out a reactor bank i that is active, and denote b_i as the cost of switching out a capacitor bank i that is active or switching in a reactor bank i that is inactive. Let $O \subseteq \Omega$ be the set of capacitor banks that are currently active and reactor banks that are inactive, and $F \subseteq \Omega$

be the set of capacitor banks that are inactive and reactor banks that are active.

The centralized controller exerts control by selecting a set $O' \subseteq \Omega$ consisting of capacitors that should be active and reactors that should be inactive. This set O' can be interpreted as a set of capacitor/reactor banks that are selected to inject reactive power to the buses where they are located. Based on the current status set O and decision set O' , the actual control action is to switch a set of capacitor/reactor banks, denoted as $S \subseteq \Omega$, from on to off or from off to on with $S = (O' \setminus O) \cup (O \setminus O')$.

The goal of the centralized controller is to choose the injecting set O' that minimizes the resulting voltage deviations at PQ buses and the operating cost. The cost of voltage deviation and operation can be captured by the metric $f(O')$, defined as

$$f(O') = \sum_{j \in O' \setminus O} c_j + \sum_{j \in O \setminus O'} b_j + \lambda \sum_{i=1}^n h(V_i + \Delta V_i - V_{ref,i}), \quad (6)$$

where h is a penalty function on voltage deviation at PQ buses. The function h is chosen to be convex as heavier penalty should be applied if the voltage deviates further from the reference. The first two terms in Equation (6) give the total operating cost of switching capacitor/reactor banks in S , while the third term is a sum of penalties on voltage deviations at each PQ bus after switching capacitor/reactor banks in S . λ is a nonnegative trade-off factor between the operating cost and the penalty on voltage deviations.

By using the approximation of Eq. (3), the last term of Eq. (6) can be re-written as

$$\lambda \sum_{i=1}^n h \left(\sum_{j \in S} \omega_{ij} (\Delta Q_j) - V_{ref,i} + V_i \right),$$

where $\omega_{ij} = D_{ik}$ for $j \in \Omega_k$, i.e., the capacitor/reactor bank $j \in S$ located at bus k . (Here, D_{ik} denotes the i th row and k th column entry of the matrix D in Section III-A.) The parameter, ω_{ij} , can be interpreted as the approximated incremental increase in voltage at bus i from a per unit reactive power injection by capacitor/reactor bank j .

By substituting S with $(O' \setminus O) \cup (O \setminus O')$ and rearranging terms, we have

$$f(O') = \sum_{j \in O' \setminus O} c_j + \sum_{j \in O \setminus O'} b_j + \lambda \sum_{i=1}^n h \left(\sum_{j \in O'} \omega_{ij} |\Delta Q_j| - \bar{V}_i \right), \quad (7)$$

where $\bar{V}_i = V_{ref,i} - V_i + \sum_{j \in O} \omega_{ij} |\Delta Q_j|$. The problem of selecting an optimal set O' of capacitor/reactor banks to inject reactive power can then be formulated as a discrete optimization problem

$$\min \{f(O') : O' \subseteq \Omega\}. \quad (8)$$

This is a combinatorial optimization problem, and hence cannot be efficiently solved or approximated unless the objective function possesses additional structure, such as submodularity. While the objective function $f(O')$ is not supermodular, an equivalent submodular objective function can still be derived, as shown in the following subsection.

B. Submodular Optimization Approach

We first give a new problem formulation with a matroid constraint, followed by the proof of its equivalence to the previous formulation. We then demonstrate that this problem has the structure of matroid basis-constrained submodular maximization. The submodular formulation is established on an expanded ground set $\bar{\Omega}$, defined as

$$\bar{\Omega} = \{v_{jl} : j \in \Omega, l = 0, 1\},$$

where v_{j0} denotes the event that the capacitor bank j is inactive (or active if j is reactor bank), while v_{j1} is the event that the capacitor bank j is active (or inactive for reactor bank).

For each PQ bus i , let $P_i = \{j \in \Omega : \omega_{ij} > 0\}$ and $R_i = \{j \in \Omega : \omega_{ij} < 0\}$, i.e., the set of capacitor/reactor banks that, by injecting reactive power at its located bus, causes an increase (P_i) or decrease (R_i) in voltage at bus i . For any set $A \subseteq \bar{\Omega}$, we define sets A_0 and A_1 by

$$A_0 = \{j \in \Omega : v_{j0} \in A\}, \quad A_1 = \{j \in \Omega : v_{j1} \in A\}.$$

The submodular formulation consists of an objective function $\hat{f} : 2^{\bar{\Omega}} \rightarrow \mathbb{R}$ that is supermodular and equivalent to Eq. (8), and a matroid constraint with the matroid bases collection denoted as \mathcal{B} . For each PQ bus i , we define a cost function $\hat{f}_i : 2^{\bar{\Omega}} \rightarrow \mathbb{R}$ by

$$\hat{f}_i(A) = h \left(\sum_{j \in P_i \cap A_1} \omega_{ij} |\Delta Q_j| + \sum_{j \in R_i \cap A_0} |\omega_{ij}| |\Delta Q_j| - \hat{V}_i \right),$$

where $\hat{V}_i = \bar{V}_i - \sum_{j \in R_i} \omega_{ij} |\Delta Q_j|$. Considering n PQ buses overall, then the system-wide cost function \hat{f} is defined as

$$\hat{f}(A) = \sum_{j \in A_1 \cap F} c_j + \sum_{j \in A_0 \cap O} b_j + \lambda \sum_{i=1}^n \hat{f}_i(A). \quad (9)$$

The equivalence between $\hat{f}(A)$ and the objective function in the previous subsection is established by the following lemma.

Lemma 3. *Suppose that the set $A \subseteq \bar{\Omega}$ satisfies $|A \cap \{v_{j0}, v_{j1}\}| = 1$ for all $j \in \Omega$. Then $\hat{f}(A) = f(A_1)$.*

The proof can be found in the appendix and it follows from the fact that, under the assumption on A , $\Omega = A_0 \cup A_1$ is a partition of the set Ω , and hence $R_i = (R_i \cap A_0) \cup (R_i \cap A_1)$ and $R_i \cap A_1 = R_i \setminus (R_i \cap A_0)$.

By Lemma 3, the problem (8) of selecting a set of buses to inject reactive power is equivalent to minimizing $\hat{f}(A)$ subject to the constraint that $|A \cap \{v_{j0}, v_{j1}\}| = 1$ for all $j \in \Omega$. We define a collection \mathcal{B} of subsets of $\bar{\Omega}$ by $A \in \mathcal{B}$ iff $|A \cap$

$\{|v_{j0}, v_{j1}\}| = 1$ for all $j \in \Omega$. Then the equivalent discrete optimization problem can be formulated as

$$\min \{\hat{f}(A) : A \in \mathcal{B}\}. \quad (10)$$

Next, we show \mathcal{B} is the collection of bases of a matroid and hence the condition that $A \in \mathcal{B}$ in Eq. (10) is a matroid basis constraint on the set $A \subseteq \bar{\Omega}$. The intuition comes from the fact that each device can be either on or off, which corresponds to $|A \cap \{v_{j0}, v_{j1}\}| = 1$ for all $j \in \Omega$, i.e., $A \in \mathcal{B}$. As a result, for any optimal selection A , the resulting A_0 and A_1 should always form a partition of Ω .

We define $\bar{\Omega}_j = \{v_{j0}, v_{j1}\}$ for $j \in \Omega$. Then the sets $\bar{\Omega}_{j \in \Omega}$ form a partition of Ω , i.e., $\bar{\Omega} = \cup_{j \in \Omega} \bar{\Omega}_j$ and $\bar{\Omega}_i \cap \bar{\Omega}_j = \emptyset$ for $i \neq j$. By Lemma 1, the constraint $A \in \mathcal{I}$ iff $|A \cap \bar{\Omega}_j| \leq 1$ for all $j \in \Omega$ defines a partition matroid $\mathcal{M} = (\bar{\Omega}, \mathcal{I})$. The bases of \mathcal{M} are the sets A satisfying $|A \cap \bar{\Omega}_j| = 1$ for all $j \in \Omega$, which are exactly the sets in \mathcal{B} .

It remains to show $\hat{f}(A)$ is supermodular, which is established by the following theorem.

Theorem 1. *The function $\hat{f}(A)$ is supermodular in $A \subseteq \bar{\Omega}$.*

The proof, which is in the appendix, is established by showing $\hat{f}(A)$ as a composition of a convex function over a non-negative modular function.

Combining Theorem 1 with the above discussion of \mathcal{B} , we have that Eq. (10) is a supermodular minimization problem, which can be transformed to an equivalent submodular maximization problem, subject to a matroid basis constraint. The submodularity of this problem allows constructing approximation algorithms with provable optimality bound, as presented in the following subsection.

C. Voltage Control Algorithms

We now present a voltage control algorithm that is derived from techniques for maximizing a submodular function subject to a matroid basis constraint.

As the constraint $A \in \mathcal{B}$ in Eq. (10) implies that each capacitor/reactor bank $j \in \Omega$ can be either active v_{1j} or inactive v_{0j} , the algorithm proceeds as follows. We initialize a set $A \subseteq \bar{\Omega}$ by the current configuration of capacitor/reactor banks such that $A = \{v_{j1} : j \in O\} \cup \{v_{j0} : j \in F\}$. For a chosen constant parameter $\epsilon > 0$, the algorithm iteratively selects a capacitor/reactor bank j from A_0 or A_1 such that

$$\hat{f}(A \setminus \{v_{j0}\} \cup \{v_{j1}\}) < (1 - \epsilon)\hat{f}(A) \text{ if } v_{j0} \in A \text{ (i.e., } j \in A_0),$$

or

$$\hat{f}(A \setminus \{v_{j1}\} \cup \{v_{j0}\}) < (1 - \epsilon)\hat{f}(A) \text{ if } v_{j1} \in A \text{ (i.e., } j \in A_1).$$

The algorithm terminates when no such device j can be found. A pseudocode description is given as Algorithm 1.

Intuitively, at each iteration, the algorithm identifies a capacitor/reactor bank $j \in \Omega$ such that switching it will reduce the system-wide cost $\hat{f}(A)$.

The algorithm converges to a ϵ -local minimum, defined as a set $A \subseteq \bar{\Omega}$ that satisfies $(1 - \epsilon)\hat{f}(A) < \hat{f}(A \cup \{v\} \setminus \{w\})$ for any $v, w \in \bar{\Omega}$ such that $(A \cup \{v\} \setminus \{w\}) \in \mathcal{B}$. The

Algorithm 1 Algorithm for selecting a set of capacitor/reactor banks to inject reactive power.

```

1: procedure SUBMODULARVC( $\mathbf{v}, \mathbf{v}_{\text{ref}}, \boldsymbol{\omega}, \mathbf{q}, \mathbf{b}, \mathbf{c}, O, F$ )
2:   Input: Initial voltages at each bus  $\mathbf{v}$ , reference voltages for PQ buses  $\mathbf{v}_{\text{ref}}$ , weights  $\omega_{ij}$  from inverse Jacobian  $J^{-1}$ , possible reactive power injections by each capacitor/reactor bank  $\mathbf{q} = \{|\Delta Q_j|, j \in \Omega\}$ , switching costs  $\mathbf{b}$  and  $\mathbf{c}$ , set of active capacitor banks and inactive reactor banks  $O$  that initially injecting reactive power,  $F = \Omega \setminus O$ .
3:   Output: Set of capacitor/reactor banks  $O'$  to inject reactive power.
4:   Initialization:  $A \leftarrow \{v_{j0} : j \in F\} \cup \{v_{j1} : j \in O\}$ ,  $A_0 \leftarrow F$ ,  $A_1 \leftarrow O$ ,  $flag = 1$ 
5:   while  $flag == 1$  do
6:      $flag = 0$ ,  $\Delta \hat{f}_0 = 0$ ,  $\Delta \hat{f}_1 = 0$ 
7:     if there exists  $j_0 \in A_0$  with  $\hat{f}(A \setminus \{v_{j_0 0}\} \cup \{v_{j_0 1}\}) < (1 - \epsilon)\hat{f}(A)$  then
8:        $j_0 \leftarrow \arg \min_{j \in A_0} \hat{f}(A \setminus \{v_{j_0 0}\} \cup \{v_{j_0 1}\})$ 
9:        $flag = 1$ ,  $\Delta \hat{f}_0 = \hat{f}(A \setminus \{v_{j_0 0}\} \cup \{v_{j_0 1}\})$ 
10:    end if
11:    if there exists  $j_1 \in A_1$  with  $\hat{f}(A \setminus \{v_{j_1 1}\} \cup \{v_{j_1 0}\}) < (1 - \epsilon)\hat{f}(A)$  then
12:       $j_1 \leftarrow \arg \min_{j \in A_1} \hat{f}(A \setminus \{v_{j_1 1}\} \cup \{v_{j_1 0}\})$ 
13:       $flag = 1$ ,  $\Delta \hat{f}_1 = \hat{f}(A \setminus \{v_{j_1 1}\} \cup \{v_{j_1 0}\})$ 
14:    end if
15:    Compare  $\Delta \hat{f}_0$  and  $\Delta \hat{f}_1$ 
16:    if  $\Delta \hat{f}_0 < \Delta \hat{f}_1$  then
17:       $A \leftarrow A \setminus \{v_{j_0 0}\} \cup \{v_{j_0 1}\}$ 
18:       $A_1 \leftarrow A_1 \cup \{j_0\}$ ,  $A_0 \leftarrow A_0 \setminus \{j_0\}$ 
19:    else if  $\Delta \hat{f}_0 > \Delta \hat{f}_1$  then
20:       $A \leftarrow A \setminus \{v_{j_1 1}\} \cup \{v_{j_1 0}\}$ 
21:       $A_0 \leftarrow A_0 \cup \{j_1\}$ ,  $A_1 \leftarrow A_1 \setminus \{j_1\}$ 
22:    end if
23:  end while
24:  if  $\hat{f}(A) \leq \hat{f}(\bar{\Omega} \setminus A)$  then
25:     $O' \leftarrow A_1$ , return  $O'$ 
26:  else
27:     $O' \leftarrow \Omega \setminus A_1$ , return  $O'$ 
28:  end if
29: end procedure

```

local minimum is known to be within a factor of $1/6$ for the nonmonotone submodular maximization problem with matroid basis constraint [24]. This optimality bound can be improved by $1/3$ by exploiting the partition matroid structure of (10), as shown in the following theorem.

Theorem 2. *Let M satisfy $\hat{f}(A) \leq M$ for all $A \subseteq \bar{\Omega}$. Define O' to be the set chosen by Algorithm 1, and let O^* be the optimal solution to $\min \{f(O') : O' \subseteq \Omega\}$. Then*

$$M - f(O') \geq \left(\frac{1}{3 + \epsilon} \right) (M - f(O^*)). \quad (11)$$

Denote the cardinality $|\Omega|$ by N . The complexity of Algorithm 1 is described by the following proposition.

Proposition 1. *Let $f_{\min} = \min \{f(O') : O' \subseteq \Omega\}$ and $f_{\max} = \max \{f(O') : O' \subseteq \Omega\}$. The runtime of the algorithm*

is bounded above by $O(NT_0)$, where $T_0 = \lceil \frac{\log \left[\frac{f_{min}}{f_{max}} \right]}{\log(1-\epsilon)} \rceil$.

The proofs for Theorem 2 and Proposition 1 can be found in the appendix.

D. Adaptive Selection Algorithm

The approach of Algorithm 1 introduces additional errors due to the approximation resulting from the linearization of the nonlinear power flow equations (1)–(2). In what follows, we present an adaptive approach that reduces these errors. Instead of using fixed values of ΔQ and the Jacobian matrix J , the adaptive algorithm solves the power flow equations at each iteration after selecting a capacitor/reactor bank to switch. The values of J and ΔQ are updated based on the new operating point. Algorithm 2 embodies this adaptive approach.

Algorithm 2 Algorithm for adaptively selecting a set of capacitor/reactor banks to inject reactive power.

```

1: procedure ADAPTIVE_VC( $\mathbf{v}$ ,  $\mathbf{v}_{ref}$ ,  $\omega$ ,  $\mathbf{q}$ ,  $\mathbf{b}$ ,  $\mathbf{c}$ ,  $O$ ,  $F$ )
2:   Line 2 – 14 in Algorithm 1
3:   Compare  $\Delta \hat{f}_0$  and  $\Delta \hat{f}_1$ 
4:   if  $\Delta \hat{f}_0 < \Delta \hat{f}_1$  then
5:      $A \leftarrow A \setminus \{v_{j_0 0}\} \cup \{v_{j_0 1}\}$ 
6:      $A_1 \leftarrow A_1 \cup \{j_0\}$ ,  $A_0 \leftarrow A_0 \setminus \{j_0\}$ 
7:     [Switch  $j_0$  and update  $\hat{f}$ : voltages  $\mathbf{v}$ ;  $O = A_1$  and
       $F = A_0$ ; Jacobian inverse matrix  $J^{-1}$  and weights  $\omega$ ]
8:   else if  $\Delta \hat{f}_0 > \Delta \hat{f}_1$  then
9:      $A \leftarrow A \setminus \{v_{j_1 1}\} \cup \{v_{j_1 0}\}$ 
10:     $A_0 \leftarrow A_0 \cup \{j_1\}$ ,  $A_1 \leftarrow A_1 \setminus \{j_1\}$ 
11:    [Switch  $j_1$  and Update  $\hat{f}$ : voltages  $\mathbf{v}$ ;  $O = A_1$  and
       $F = A_0$ ; Jacobian inverse matrix  $J^{-1}$  and weights  $\omega$ ]
12:   end if
13:   Line 23 – 28 in Algorithm 1
14:   return  $O'$ 
15: end procedure

```

Algorithm 2 proceeds with a logic similar to Algorithm 1. At each iteration, the algorithm selects a device $j \in \Omega$, such that switching device j will lower the cost function $\hat{f}(A)$. Before entering the next iteration, the centralized controller implements this switching action in simulation, and updates the cost function \hat{f} by requesting the post-switching system state from the nonlinear power flow solver.

Compared to Algorithm 1, Algorithm 2 requires one extra step at each iteration for solving the power flow equations, denoted by $F(x) = 0$. If the nonlinear power flow solver uses Newton-Raphson iterative method, provided that a good initial guess is known, then it adds a complexity of $O((\log k)H(k))$ to each iteration of Algorithm 2, where $H(k)$ is the cost of calculating $F(x)/F'(x)$ with k -digit precision. Thus, the overall computational complexity of Algorithm 2 is $O((N + O((\log k)H(k)))T_0)$.

V. CASE STUDY: 300-BUS TRANSMISSION SYSTEM

This section presents test results of our proposed voltage controller on the IEEE 300-bus test system. A state-of-the-art

algorithm [4] based on voltage sensitivities to reactive power changes is also implemented for comparison.

A. Test Setup

Power system state information (including voltage magnitudes V and angles θ) is obtained by solving power flows using Matpower [25]. Initial power flow data for the IEEE 300-bus test system is provided by the program default function `case300.m` and all test cases considered in this section are generated from this base case with variations in power demands. A power flow solution of the original `case300.m` produces an unrealistic voltage profile with a number of voltages both above and below the acceptable $[0.95, 1.05]$ per unit voltage range.

Because an optimal power flow (OPF) is not able to find a feasible solution for the original loading conditions, the following procedure was used to create realistic low voltage initial conditions. We obtain an initial operating point by scaling the active and reactive loads in the original data by a factor $\alpha < 1$. We then solve the OPF to get all bus voltages within the range $V_{min}^{opf} = 0.95$ to $V_{max}^{opf} = 1.05$. Finally we scale the active and reactive loads by a factor $\beta > 1$ at each PQ bus and solve the power flow equations. A larger β value corresponds to an increase in loading and hence additional violations of the lower voltage limit. The following parameter values were used:

- 1) Case 1: $\alpha = 0.89, \beta = 1.07$.
- 2) Case 2: $\alpha = 0.89, \beta = 1.08$.

Once an initial operating point was created, we initialized the rest of the simulation as follows. The reference voltages at PQ buses were set to $\mathbf{v}_{ref} = \mathbf{1}$ p.u.. We assume that a capacitor bank is available at each PQ bus. The IEEE 300-bus system consists of a main transmission network with high nominal voltages (66-345 kV) and a small part (buses labeled 9001-9533 in `case300.m`) with low nominal voltages (0.6-13.8 kV). Thus, two types of capacitor banks are assumed to be installed at different PQ buses. Capacitors in the main transmission network are assumed to have capacitance $C = 0.003 \text{ Mvar/kV}^2$ (e.g., 155-Mvar capacitor bank at 230 kV, [4]), while capacitors at the low-voltage branch have capacitance $C = 0.03 \text{ Mvar/kV}^2$ (e.g., 6-Mvar capacitor bank at 13.8 kV, [26]). We do not consider reactors in this simulation. We assume that no capacitor banks are energized at the initial operating point, i.e., $O = \emptyset$.

All algorithms are implemented in MatlabTM. Given necessary information including the initial voltages, corresponding Jacobian matrix and capacitances of capacitor banks, each algorithm returns a set S of buses where reactive power will be injected.

The total cost $f(S)$ of any switching action S is calculated using Eq. (6). We choose a trade-off factor $\lambda = 1$. For switching costs at bus i , we set $b_i = 1$ and $c_i = 1$ for switching capacitor banks off and on, respectively. The parameters used in cost function f are chosen to make the switching costs relatively small compared to penalties on the voltage deviation, such that switching solutions are differentiated mainly by their impact on the voltage.

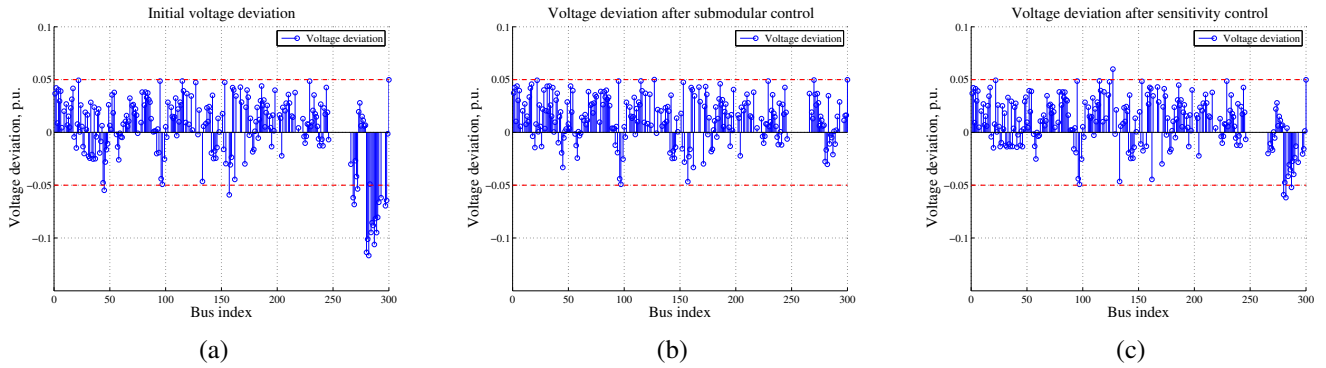


Fig. 1: Comparing submodular voltage control with sensitivity-based voltage control in test case 1. (a) Initial voltage deviation. Initially, 19 buses are below the desired operating voltage. (b) Effect of the submodular control algorithm on system voltages. After exerting control, one bus is at 1.05 p.u. and no bus is below 0.95 p.u.. (c) Change in voltage due to the sensitivity voltage control. After exerting the control, 3 PQ buses have voltages below the desired operating range of $[0.95, 1.05]$ p.u..

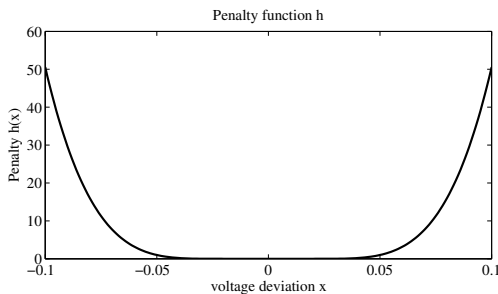


Fig. 2: Convex penalty function $h(x)$ for voltage deviation.

The convex penalty function, h , on voltage deviations from Eq. (6) is defined by

$$h(x) = \begin{cases} \left(\frac{x - V_{high}}{V_{max} - V_{high}} \right)^4, & x > V_{high} \\ 0, & V_{low} < x \leq V_{high} \\ \left(\frac{x - V_{low}}{V_{min} - V_{low}} \right)^4, & x \leq V_{low} \end{cases}$$

where $V_{low} = -0.02$ and $V_{high} = 0.02$ are the lower and upper bounds on the desired voltage region, while $V_{min} = -0.05$ and $V_{max} = 0.05$ are limits defining voltage violations (Figure 2).

For comparison, we implement the sensitivity-based control algorithm of [4], which proceeds as follows. The controller first calculates voltage sensitivities of each bus i due to a reactive power change at bus k using the Jacobian matrix J by

$$\Lambda_i = \min_j \left| \frac{\partial V_i}{\partial Q_k} / \frac{\partial V_j}{\partial Q_k} \right|, \quad 0 \leq \Lambda_i \leq 1.$$

It then divides the system topology into M control areas for M voltage violating nodes. Given any threshold Λ^* , each area k has nodes defined by the set $A_k = \{v_i : \Lambda_i > \Lambda^* \text{ for any injection at bus } k\}$. Areas are combined if they are not disjoint, $A_x \cap A_y \neq \emptyset$. In each area, the controller enumerates all possible control actions and selects the set of actions S that minimizes $f(S)$.

In the following subsections, we present the performance of submodular control Algorithm 1 and adaptive control Al-

gorithm 2, as well as the sensitivity algorithm, for the two test cases we created. Buses are labeled by integers from 1 to 300 following the order in `case300.m`. We choose the parameter $\epsilon = 0$ for both Algorithm 1 and Algorithm 2.

B. Comparison of Submodular and Sensitivity-Based Methods

Figure 1(a) shows the initial voltages prior to any control actions for test case 1. 19 PQ buses have voltages below 0.95 with a minimum voltage of 0.8834 p.u. at Bus 282. The maximum voltage is 1.0498 p.u. at Bus 300, which is within the limits. The initial operating point has a total cost $f(\emptyset) = 537.6943$.

Since the error in the linear prediction of voltage deviation is negligible, we observe that Algorithm 1 and Algorithm 2 give the same switching set $S_{sub} = \{133, 157, 270\}$, which lowers the total cost to $f(S_{sub}) = 20.4634$. After control is exerted, no bus voltage falls below 0.95 p.u., while the voltage of Bus 127 is at the upper limit (Figure 1(b)). We observe that, while 19 buses experienced low voltages, only one of them (157) was selected to inject reactive power.

For the sensitivity approach in test case 1, a threshold $\Lambda^* = 0.2$ is used as suggested in [4]. The sensitivity-based algorithm took five times as long to complete as the submodular control algorithm on a Macbook with 2.4GHz dual-core Intel Core i5 processor and 8GB RAM. The sensitivity approach identifies four areas (A_1, A_2, A_3, A_4) containing 1, 3, 5 and 18 buses, respectively. Four sets of buses, $S_1 = \{293\}$, $S_2 = \{44, 45, 48\}$, $S_3 = \{124, 157, 158, 159\}$, and $S_4 = \{268, 269, 271, 272, 285, 290, 291\}$ are selected to inject reactive power in areas A_1, A_2, A_3 and A_4 , respectively (Figure 1(c)). This control solution ($S_{sens} = S_1 \cup S_2 \cup S_3 \cup S_4$) results in 3 PQ buses with voltage below 0.95 p.u. while 1 bus (127) has a voltage of 1.0599 p.u., which is above the upper limit. The total cost has been lowered to $f(S_{sens}) = 40.9636$.

An intuitive explanation for the different outcomes of the submodular and sensitivity-based algorithms is as follows. In order to reduce computation time, the sensitivity algorithm partitions the power system into regions around buses with voltage violations, and attempts to find a set of reactive power injections within each region to resolve any voltage deviations.

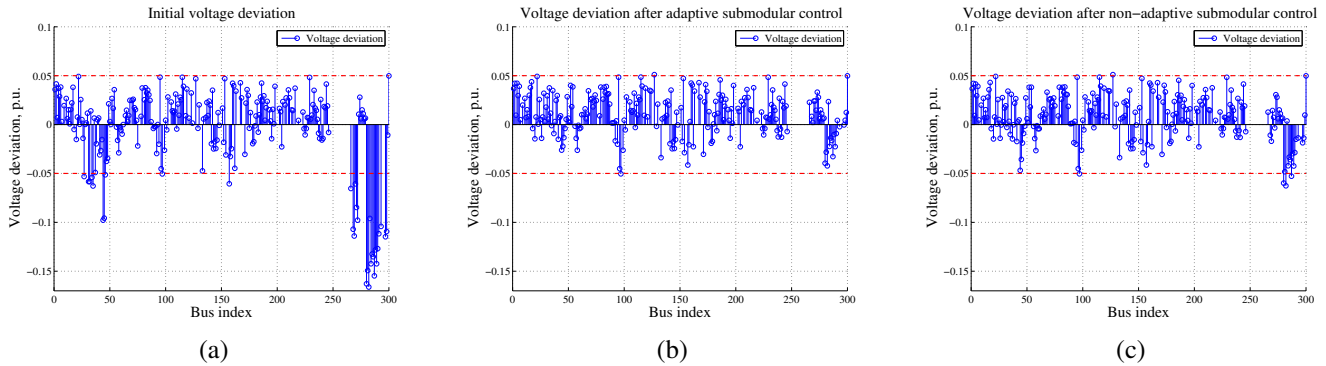


Fig. 3: Comparing adaptive submodular and non-adaptive submodular voltage control in test case 2. (a) Initial voltage deviation. Initially, 31 buses are below the desired operating voltage. (b) Effect of the adaptive submodular control algorithm on system voltages. After exerting control, 1 bus is above 1.05 p.u. and 1 bus is below 0.95 p.u.. (c) Effect of the non-adaptive submodular control algorithm on system voltages. After exerting control, 1 bus is above 1.05 p.u. and 4 buses are below 0.95 p.u..

In this case, however, any additional switching actions beyond S_4 within region A_4 results in a minor reduction in voltage deviation at a high switching cost. The sensitivity algorithm therefore selects S_4 as the local optimal control actions within this region. On the other hand, our submodular control algorithm restores the voltages to the desired range by selecting devices outside the region A_4 to inject reactive power. In summary, this test case suggests that the submodular algorithm provides a better performance than sensitivity-based algorithm when different areas of the grid are highly interdependent. This is because an optimal strategy has to take into account local voltage deviations as well as the coupling between areas.

C. Comparison of Non-Adaptive and Adaptive Algorithms

We now compare the performance of the adaptive control algorithm (Algorithm 2) with the non-adaptive algorithm (Algorithm 1) in test case 2. The initial operating point has 31 buses with low voltages, including a minimum voltage of 0.8338 p.u.. Voltages at the other buses are within range, with a maximum voltage of 1.0498 p.u.. Before taking any control actions, the initial total cost is $f(\emptyset) = 3853.8877$.

This is a much more heavily loaded operating point compared to test case 1. Buses 280, 282 and 287 have voltages that drop below 0.85 p.u., which must be mitigated through reactive power injection. We set $\epsilon = 0$ for both the non-adaptive Algorithm 1 and the adaptive Algorithm 2. A large threshold $\Lambda^* = 0.92$ is used for the sensitivity algorithm, which divides the system into 10 areas with a maximum area size of 17 buses. This value of the threshold is chosen to limit the number of buses in the largest control area to a reasonable amount. Table I shows the control actions and the resulting costs. While all algorithms significantly reduce the total voltage deviations, Table II shows that the submodular algorithms (Algorithm 1 and 2) achieve better voltage profiles than the sensitivity-based controller. Figure 3 illustrates the performance of adaptive Algorithm 2 compared to non-adaptive Algorithm 1. We observe that the adaptive algorithm provides better performance due to a more accurate prediction of voltage deviations in the heavy loading case.

TABLE I: Comparison of control actions selected by adaptive submodular, non-adaptive submodular, and sensitivity-based algorithms in test case 2

Algorithms	Buses selected to inject reactive power, S	Total cost, $f(S)$ (initial 3853.8877)
Adaptive	{31,44,45,124,162,266,268}	21.0875
Non-adaptive	{45,124,162,266}	27.8693
Sensitivity	{27,32,34,35,44,45,46,157,269,272,280,281,282,283,284,285,286,287,288,289,290,291,293,297,298}	184.2068

TABLE II: Voltage profile after exerting control under adaptive submodular, non-adaptive submodular, and sensitivity-based algorithms in test case 2

Algorithms	Number of buses with low voltage (below 0.95 p.u.)	Number of buses with high voltage (above 1.05 p.u.)	Lowest voltage	Highest voltage
Adaptive	1	1	0.9496	1.0510
Non-adaptive	4	1	0.9374	1.0510
Sensitivity	11	0	0.9053	1.0498

D. Voltage Control Following Generator Tripping

Any change in system topology, such as a generator or transmission line tripping, could also cause low voltages ($V < 0.95$ p.u.). This is because after rebalancing the generation and load following the topology change, the total reactive power loss may increase, for example, due to more power flows on high inductance transmission lines. This subsection presents a test of the proposed submodular voltage control algorithm on an initial operating point that has dozens of buses experiencing low voltage following a generator tripping, with a comparison to the sensitivity-based control algorithm. The goal of this test is to demonstrate the ability of our proposed submodular voltage control algorithms to correct voltage deviations arising from a system topology change.

As in the previous two test cases, the initial operating point for this test case is obtained from the IEEE 300-bus system by scaling the active and reactive loads in the original data `case300.m` down by the factor $\alpha = 0.89$. The OPF solution shows that all bus voltages are then within the range $V_{\min}^{opf} = 0.95$ to $V_{\max}^{opf} = 1.05$ p.u.. All other parameters and

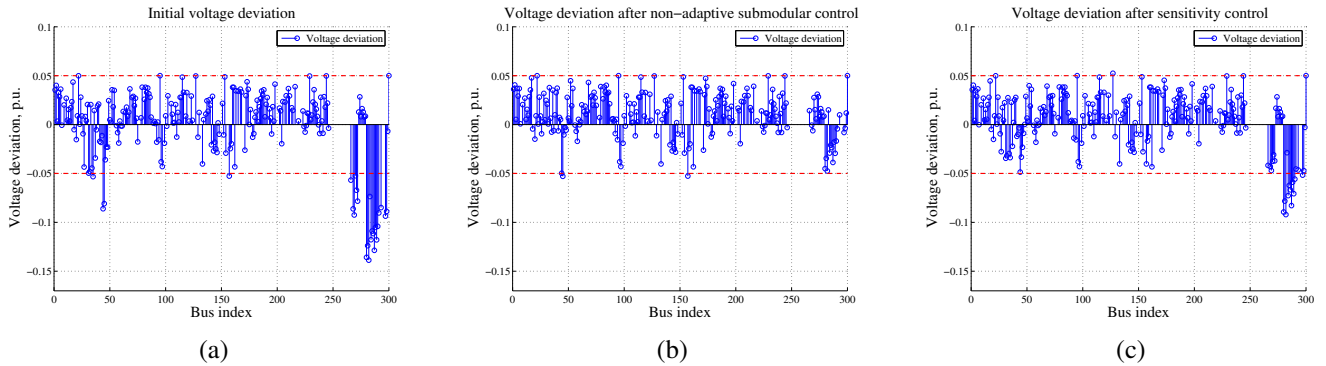


Fig. 4: Comparing submodular voltage control and sensitivity-based voltage control in generator tripping case. (a) Initial voltage deviation. In total, 25 buses are below the desired operating voltage. (b) Effect of the submodular control algorithm on system voltages. After exerting control, no bus is above 1.05 p.u. and 2 buses are below 0.95 p.u.. (c) Change in voltage due to the sensitivity voltage control. After exerting control, 1 bus is above 1.05 p.u. and 11 buses are below 0.95 p.u..

assumptions are the same as in the previous test cases.

The generator at Bus 165 is chosen to be tripped. Without load shedding, the resulting loss in active power is fully compensated by the slack bus. After this generator tripping, a power flow solution produces a voltage profile with 25 buses having voltages below 0.95, the lowest voltage being 0.8614 p.u. These low voltages occur due to an increase in reactive power losses from 3972.5 Mvar to 5641.6 Mvar throughout the grid. Before exerting any controls, the voltage deviations resulting from the generator tripping incur a total cost $f(\emptyset) = 1564.8701$.

We select the same parameters for algorithms as in test case 2, in order to limit the computational times of the different algorithms to a comparable amount. For both the non-adaptive Algorithm 1 and the adaptive Algorithm 2, we set $\epsilon = 0$. For the sensitivity algorithm, the threshold $\Lambda^* = 0.92$ is used, which divides the power system into 5 areas with a maximum area size of 17 buses. In this test case, the sensitivity-based algorithm requires at least three times the computing time required by the submodular control algorithms.

Table III lists the buses selected for reactive power injection and the resulting cost for each algorithm. The detailed voltage profile after exerting control with each algorithm is given in Table IV. We observe that the submodular voltage control algorithms select fewer buses to inject reactive power but results in a solution with more buses returning to the normal operating region compared with the sensitivity algorithm. In particular, both the adaptive submodular algorithm and non-adaptive submodular algorithm are able to find a “key” bus, Bus 270, where injecting reactive power can mitigate voltage deviations at most buses. The voltage at this bus, however, is less sensitive to its own reactive power injection compared to its effect on some other buses. Because a large threshold $\Lambda^* = 0.92$ is used to ensure that the sensitivity algorithm is computationally feasible, Bus 270 is excluded from the control area in this case. Although a large number of buses are selected, the sensitivity-based algorithm cannot effectively reduce the voltage deviations at all buses compared to the submodular algorithms.

Figure 4 demonstrates the shift of voltages at all PQ buses

with the non-adaptive submodular and the sensitivity-based algorithms. We observe that in the case of tripping a generator at Bus 165, the proposed submodular voltage control can achieve better voltage profiles compared to the sensitivity approach.

TABLE III: Comparison of control actions selected by the adaptive submodular, non-adaptive submodular, and sensitivity-based algorithms after generator tripping.

Algorithms	Buses selected to inject reactive power, S	Total cost, $f(S)$ (initial 3853.8877)
Adaptive	{44,270}	19.1012
Non-adaptive	{270}	20.5082
Sensitivity	{35,44,45,157,269,272,280,281,282,283,284,285,286,287,288,289,290,291,293}	165.4577

TABLE IV: Voltage profile after exerting control with the adaptive submodular, non-adaptive submodular, and sensitivity-based algorithms after generator tripping.

Algorithms	Number of buses with low voltage (below 0.95 p.u.)	Number of buses with high voltage (above 1.05 p.u.)	Lowest voltage	Highest voltage
Adaptive	1	0	0.9473	1.0500
Non-adaptive	2	0	0.9471	1.0510
Sensitivity	11	1	0.9080	1.0524

VI. CONCLUSION

This paper proposed computationally efficient centralized voltage control algorithms with provable optimality bounds that are scalable to large power systems. It presented a discrete optimization approach for selecting a subset of reactive power injection devices to minimize switching costs and voltage deviations from desired levels. We proved that this formulation is equivalent to submodular maximization with a matroid basis constraint, leading to efficient approximation algorithms with provable bounds. The algorithms were evaluated numerically on the IEEE 300-bus transmission system and compared to an existing voltage control algorithm. We found that our proposed submodular control approach achieves voltage profiles with less voltage deviation in the same computation time.

APPENDIX

Proof of Lemma 3. The proof contains two parts. First, the condition $|A \cap \{v_{j0}, v_{j1}\}| = 1$ for all $j \in \Omega$ implies $\Omega = A_0 \cup A_1$ and hence we have

$$\sum_{j \in A_1 \setminus O} c_j + \sum_{j \in O \setminus A_1} b_j = \sum_{j \in A_1 \setminus O} c_j + \sum_{j \in A_0 \cap O} b_j.$$

Then it suffices to show that, for each PQ bus i ,

$$\hat{f}_i(A) = h \left(\sum_{j \in A_1} \omega_{ij} |\Delta Q_j| - \bar{V}_i \right)$$

when the condition $|A \cap \{v_{j0}, v_{j1}\}| = 1$ holds for all $j \in \Omega$. We have

$$\begin{aligned} \sum_{j \in A_1} \omega_{ij} |\Delta Q_j| &= \sum_{j \in A_1 \cap P_i} \omega_{ij} |\Delta Q_j| + \sum_{j \in A_1 \cap R_i} \omega_{ij} |\Delta Q_j| \\ &= \sum_{j \in A_1 \cap P_i} \omega_{ij} |\Delta Q_j| + \sum_{j \in R_i} \omega_{ij} |\Delta Q_j| \quad (12) \\ &\quad - \sum_{j \in R_i \cap A_0} \omega_{ij} |\Delta Q_j|, \end{aligned}$$

where (12) follows from the fact that, under the assumption on A , $\Omega = A_0 \cup A_1$ is a partition of the set Ω , and hence $R_i = (R_i \cap A_0) \cup (R_i \cap A_1)$ and $R_i \cap A_1 = R_i \setminus (R_i \cap A_0)$. Then

$$\begin{aligned} &h \left(\sum_{j \in A_1} \omega_{ij} |\Delta Q_j| - \bar{V}_i \right) \\ &= h \left(\sum_{j \in A_1 \cap P_i} \omega_{ij} |\Delta Q_j| + \sum_{j \in A_0 \cap R_i} |\omega_{ij}| |\Delta Q_j| \right. \\ &\quad \left. - \left[\bar{V}_i - \sum_{j \in R_i} \omega_{ij} |\Delta Q_j| \right] \right) = \hat{f}_i(A), \end{aligned}$$

as desired. \square

Proof of Theorem 1. The approach of the proof is to show a more general result, namely, that any function $g(A)$ defined by $g(A) = h \left(\sum_{j \in A} \alpha_j - \beta \right)$, where $\alpha_j \geq 0$ and $\beta \in \mathbb{R}$, is supermodular as a function of A . Define $\rho = \frac{\sum_{j \in A \setminus B} \alpha_j}{\sum_{j \in A \Delta B} \alpha_j}$, where Δ is the symmetric difference operator. Since all α_j 's are nonnegative, $\rho \in [0, 1]$. We have

$$\begin{aligned} \sum_{j \in A} \alpha_j &= \rho \sum_{j \in A \cup B} \alpha_j + (1 - \rho) \sum_{j \in A \cap B} \alpha_j, \\ \sum_{j \in B} \alpha_j &= (1 - \rho) \sum_{j \in A \cup B} \alpha_j + \rho \sum_{j \in A \cap B} \alpha_j. \end{aligned}$$

By substitution, we have

$$\begin{aligned} g(A) + g(B) &= h \left(\sum_{j \in A} \alpha_j - \beta \right) + h \left(\sum_{j \in B} \alpha_j \right) \\ &= h \left(\rho \left(\sum_{j \in A \cup B} \alpha_j - \beta \right) + (1 - \rho) \left(\sum_{j \in A \cap B} \alpha_j - \beta \right) \right) \\ &\quad + h \left((1 - \rho) \left(\sum_{j \in A \cup B} \alpha_j - \beta \right) + \rho \left(\sum_{j \in A \cap B} \alpha_j - \beta \right) \right) \\ &\leq \rho h \left(\sum_{j \in A \cup B} \alpha_j - \beta \right) + (1 - \rho) h \left(\sum_{j \in A \cap B} \alpha_j - \beta \right) \\ &\quad + (1 - \rho) h \left(\sum_{j \in A \cup B} \alpha_j - \beta \right) + \rho h \left(\sum_{j \in A \cap B} \alpha_j - \beta \right) \\ &= g(A \cup B) + g(A \cap B), \end{aligned}$$

which establishes the supermodularity of g .

Since the function $\hat{f}_i(A)$ can be obtained from $g(A)$ by setting $\alpha_j = |\omega_{ij}| |\Delta Q_j|$ and $\beta = \bar{V}_i$, each $\hat{f}_i(A)$ is supermodular. The terms $\sum_{i \in A_1 \setminus O} c_i + \sum_{i \in A_0 \cap O} b_i$ can be shown to be modular. The function $\hat{f}(A)$ is therefore a sum of supermodular and modular functions, and hence is supermodular. \square

Proof of Theorem 2. Let $A^* = \{v_{i1} : i \in O^*\} \cup \{v_{i0} : i \in \Omega \setminus O^*\}$ and $A = \{v_{i1} : i \in O'\} \cup \{v_{i0} : i \in \Omega \setminus O'\}$. Define a function $\hat{g}(A) = M - \hat{f}(A)$, so that \hat{g} is a nonnegative submodular function. By Lemma 2,

$$(2 + \epsilon) \hat{g}(A) \geq \hat{g}(A \cup A^*) + \hat{g}(A \cap A^*). \quad (13)$$

From Algorithm 1, Line 22–26 implies that $\hat{f}(A) \leq \hat{f}(\bar{\Omega} \setminus A)$. Applying it to (13) yields

$$(3 + \epsilon) \hat{g}(A) \geq \hat{g}(A \cup A^*) + \hat{g}(\bar{\Omega} \setminus A) + \hat{g}(A \cap A^*). \quad (14)$$

By submodularity and nonnegativity of \hat{g} , we have

$$\begin{aligned} &\hat{g}(A \cup A^*) + \hat{g}(\bar{\Omega} \setminus A) \\ &\geq \hat{g}(A^c \cap (A \cup A^*)) + \hat{g}(A^c \cup (A \cup A^*)) \\ &= \hat{g}(\bar{\Omega}) + \hat{g}(A^* \setminus A) \geq \hat{g}(A^* \setminus A). \end{aligned}$$

Applying this inequality to (14) yields

$$\begin{aligned} (3 + \epsilon) \hat{g}(A) &\geq \hat{g}(A^* \setminus A) + \hat{g}(A \cap A^*) \\ &\geq \hat{g}(A^*) + \hat{g}(\emptyset) \geq \hat{g}(A^*) \end{aligned}$$

by submodularity of \hat{g} . By Lemma 3, $\hat{g}(A) = M - f(O')$ and $\hat{g}(A^*) = M - f(O^*)$. Substitution of \hat{g} then gives (11). \square

Proof of Proposition 1. Let O'_i denote the set O' after i iterations of the algorithm. By construction, $f(O'_i) < (1 - \epsilon) f(O'_{i-1})$, and hence $f(O'_i) < (1 - \epsilon)^i f(O'_0)$.

Let T denote the number of iterations before the algorithm terminates. By definition,

$$f_{min} \leq f(O'_T) < (1 - \epsilon)^T f(O'_0) \leq (1 - \epsilon)^T f_{max}.$$

Rearranging terms yields $T \leq T_0$. Each iteration requires at most N evaluations of the objective function $f(O')$ in order to identify a capacitor/reactor bank to activate or deactivate, implying that the computation is $O(NT_0)$ in the worst case. \square

REFERENCES

- [1] P. Kundur, *Power System Stability and Control*. McGraw-Hill New York, 1994.
- [2] L. L. Grigsby, *Power System Stability and Control*. CRC press, 2012, vol. 5.
- [3] B. Zhang, A. D. Dominguez-Garcia, and D. Tse, "A local control approach to voltage regulation in distribution networks," *North American Power Symposium (NAPS)*, pp. 1–6, 2013.
- [4] V. Venkatasubramanian, J. Guerrero, J. Su, H. Chun, X. Zhang, F. Habibi-Ashrafi, A. Salazar, and B. Abu-Jaradeh, "Hierarchical two-level voltage controller for large power systems," *IEEE Transactions on Power Systems*, vol. 31, no. 1, pp. 397–411, 2016.
- [5] I. Dobson and H.-D. Chiang, "Towards a theory of voltage collapse in electric power systems," *Systems & Control Letters*, vol. 13, no. 3, pp. 253–262, 1989.
- [6] S. Greene, I. Dobson, and F. L. Alvarado, "Contingency ranking for voltage collapse via sensitivities from a single nose curve," *IEEE Transactions on Power Systems*, vol. 14, no. 1, pp. 232–240, 1999.
- [7] P. Lagonotte, J. C. Sabonnadiere, J. Y. Leost, and J. P. Paul, "Structural analysis of the electrical system: application to secondary voltage control in France," *IEEE Transactions on Power Systems*, vol. 4, no. 2, pp. 479–486, 1989.
- [8] S. Corsi, P. Marannino, N. Losignore, G. Moreschini, and G. Piccini, "Coordination between the reactive power scheduling function and the hierarchical voltage control of the EHV ENEL system," *IEEE Transactions on Power Systems*, vol. 10, no. 2, pp. 686–694, 1995.
- [9] H. Vu, P. Pruvot, C. Launay, and Y. Harmand, "An improved voltage control on large-scale power system," *IEEE Transactions on Power Systems*, vol. 11, no. 3, pp. 1295–1303, 1996.
- [10] J. L. Sancha, J. L. Fernandez, A. Cortes, and J. T. Abarca, "Secondary voltage control: analysis, solutions and simulation results for the spanish transmission system," *IEEE Transactions on Power Systems*, vol. 11, no. 2, pp. 630–638, 1996.
- [11] T. Amraee, A. Soroudi, and A. M. Ranjbar, "Probabilistic determination of pilot points for zonal voltage control," *IET Generation, Transmission Distribution*, vol. 6, no. 1, pp. 1–10, 2012.
- [12] C.-N. Yu, Y. T. Yoon, M. D. Ilic, and A. Catelli, "On-line voltage regulation: the case of New England," *IEEE Transactions on Power Systems*, vol. 14, no. 4, pp. 1477–1484, 1999.
- [13] Y. Chen, "Development of automatic slow voltage control for large power systems," Ph.D. dissertation, Washington State University, Pullman, WA, 2001.
- [14] J. Su, "A heuristic slow voltage control scheme for large power systems," Ph.D. dissertation, Washington State University, Pullman, WA, 2006.
- [15] B. Robbins, C. N. Hadjicostis, A. D. Domínguez-García *et al.*, "A two-stage distributed architecture for voltage control in power distribution systems," *IEEE Transactions on Power Systems*, vol. 28, no. 2, pp. 1470–1482, 2013.
- [16] M. Hajian, M. Glavic, W. D. Rosehart, and H. Zareipour, "A chance-constrained optimization approach for control of transmission voltages," *IEEE Transactions on Power Systems*, vol. 27, no. 3, pp. 1568–1576, 2012.
- [17] M. Hajian, W. Rosehart, M. Glavic, H. Zareipour, and T. V. Cutsem, "Linearized power flow equations based predictive control of transmission voltages," in *46th Hawaii International Conference on System Sciences*, 2013, pp. 2298–2304.
- [18] M. Glavic, D. Novosel, E. Heredia, D. Kosterev, A. Salazar, F. Habibi-Ashrafi, and M. Donnelly, "See it fast to keep calm: Real-time voltage control under stressed conditions," *IEEE Power and Energy Magazine*, vol. 10, no. 4, pp. 43–55, 2012.
- [19] V. Tzoumas, M. A. Rahimian, G. J. Pappas, and A. Jadbabaie, "Minimal actuator placement with optimal control constraints," in *American Control Conference (ACC)*, 2015, pp. 2081–2086.
- [20] A. Clark, B. Alomair, L. Bushnell, and R. Poovendran, *Submodularity in Dynamics and Control of Networked Systems*. Springer, 2016.
- [21] Z. Liu, A. Clark, P. Lee, L. Bushnell, D. Kirschen, and R. Poovendran, "Towards scalable voltage control in smart grid: A submodular optimization approach," in *ACM/IEEE 7th International Conference on Cyber-Physical Systems (ICCP)*, 2016, pp. 1–10.
- [22] P. Sauer and M. Pai, "Power system steady-state stability and the load-flow jacobian," *IEEE Transactions on Power Systems*, vol. 5, no. 4, pp. 1374–1383, 1990.
- [23] S. Fujishige, *Submodular Functions and Optimization*. Elsevier, 2005, vol. 58.
- [24] J. Lee, V. S. Mirrokni, V. Nagarajan, and M. Sviridenko, "Maximizing nonmonotone submodular functions under matroid or knapsack constraints," *SIAM Journal on Discrete Mathematics*, vol. 23, no. 4, pp. 2053–2078, 2010.
- [25] R. D. Zimmerman, C. E. Murillo-Sanchez, and R. J. Thomas, "Matpower: Steady-state operations, planning, and analysis tools for power systems research and education," *IEEE Transactions on Power Systems*, vol. 26, no. 1, 2011.
- [26] J. C. Das, "Analysis and control of large-shunt-capacitor-bank switching transients," *IEEE Transactions on Industry Applications*, vol. 41, no. 6, pp. 1444–1451, 2005.



Zhipeng Liu (S'15) is currently a Ph.D. candidate in the Department of Electrical Engineering at the University of Washington. He received the B.S. degree in Mathematics from the City University of Hong Kong in 2013 and the M.S. degree in Applied Mathematics from the University of Washington - Seattle in 2014. His research interests include input and output selection for stabilizing control, submodular optimization, and power system stability.



Andrew Clark (M'15) is an Assistant Professor in the Department of Electrical and Computer Engineering at Worcester Polytechnic Institute. He received the B.S. degree in Electrical Engineering and the M.S. degree in Mathematics from the University of Michigan - Ann Arbor in 2007 and 2008, respectively. He received the Ph.D. degree from the Network Security Lab (NSL), Department of Electrical Engineering, at the University of Washington - Seattle in 2014. He is author or co-author of the IEEE/IFIP William C. Carter award-winning paper

(2010), the WiOpt Best Paper (2012), and the WiOpt Student Best Paper (2014), and was a finalist for the IEEE CDC 2012 Best Student-Paper Award. He holds a patent in privacy-preserving constant-time identification of RFID. His research interests include control and security of complex networks, submodular optimization, control-theoretic modeling of network security threats, and deception-based network defense mechanisms.



Phillip Lee (M'16) received the B.S. degree in Electrical Engineering from the University of Washington - Seattle in 2006 and the M.S. degree in Electrical and Computer Engineering from the University of California - San Diego in 2009. He received the Ph.D. degree from the Network Security Lab (NSL), Department of Electrical Engineering, at the University of Washington in 2016. Currently, he is a Research Scientist at Honeywell International Inc.. His research interests include control-theoretic modeling of cyber threats, as well as modeling and

design of cyberphysical systems and smart-grid security.



Linda Bushnell (F'17) is a Research Associate Professor and the Director of the Networked Control Systems Lab in the Electrical Engineering Department at the University of Washington - Seattle. She received the B.S. degree and M.S. degree in Electrical Engineering from the University of Connecticut - Storrs in 1985 and 1987, respectively. She received the M.A. degree in Mathematics and the Ph.D. degree in Electrical Engineering from the University of California - Berkeley in 1989 and 1994, respectively. She also received the MBA from

the University of Washington Foster School of Business in 2010. Her research interests include networked control systems, control of complex networks, and secure-control. She was elected a Fellow of the IEEE for her contributions to networked control systems. She is a recipient of the US Army Superior Civilian Service Award, NSF ADVANCE Fellowship, and IEEE Control Systems Society Recognition Award. She was the Co-Editor of a special issue of the Asian Journal of Control and Guest Editor for three issues of the IEEE Control Systems Magazine. For the IEEE Control Systems Society, she is a Member of the Board of Governors, a Distinguished Lecturer, a Chair of the Women in Control Standing Committee, a member of the TC Control Education, a member of the History Committee, and the Liaison to IEEE Women in Engineering. She is also the Treasurer of the American Automatic Control Council.



Daniel Kirschen (F'07) is the Donald W. and Ruth Mary Close Professor of Electrical Engineering at the University of Washington - Seattle. His research focuses on the integration of renewable energy sources in the grid, power system economics and power system resilience. Prior to joining the University of Washington, he taught for 16 years at The University of Manchester (UK). Before becoming an academic, Daniel worked for Control Data and Siemens on the development of application software for utility control centers. He holds a Ph.D from

the University of Wisconsin-Madison and an Electro-Mechanical Engineering degree from the Free University of Brussels (Belgium). He is the author of two books and a Fellow of the IEEE for his contributions to analysis of power system economics and power system security.



Radha Poovendran (F'15) is a Professor and Chair of the Electrical Engineering Department, Director of the Network Security Lab (NSL), and Associate Director of the Center for Excellence in Information Assurance Research and Education, all at the University of Washington - Seattle. He received the B.S. degree in Electrical Engineering and the M.S. degree in Electrical and Computer Engineering from the Indian Institute of Technology- Bombay and University of Michigan - Ann Arbor in 1988 and 1992, respectively. He received the Ph.D. degree

in Electrical and Computer Engineering from the University of Maryland - College Park in 1999. His research interests are in the areas of wireless and sensor network security, control and security of cyber-physical systems, adversarial modeling, smart connected communities, control-security, games-security and information theoretic security in the context of wireless mobile networks. He was elected a Fellow of the IEEE for his contributions to security in cyber-physical systems. He is a recipient of the NSA LUCITE Rising Star Award (1999), National Science Foundation CAREER (2001), ARO YIP (2002), ONR YIP (2004), and PECASE (2005) for his research contributions to multi-user wireless security. He is also a recipient of the Outstanding Teaching Award and Outstanding Research Advisor Award from the University of Washington EE (2002), Graduate Mentor Award from Office of the Chancellor at University of California - San Diego (2006), and the University of Maryland ECE Distinguished Alumni Award (2016). He was co-author of award-winning papers including IEEE/IFIP William C. Carter Award Paper (2010) and WiOpt Best Paper Award (2012).